

Extending DNN-based Multiplicative Masking to Deep Subband Filtering for Improved Dereverberation

Jean-Marie Lemercier, Julian Tobergte, Timo Gerkmann

Signal Processing (SP), Universität Hamburg, Germany

{firstname.lastname}@uni-hamburg.de

Abstract

In this paper, we present a scheme for extending deep neural network-based multiplicative maskers to deep subband filters for speech restoration in the time-frequency domain. The resulting method can be generically applied to any deep neural network providing masks in the time-frequency domain, while requiring only few more trainable parameters and a computational overhead that is negligible for state-of-the-art neural networks. We demonstrate that the resulting deep subband filtering scheme outperforms multiplicative masking for dereverberation, while leaving the denoising performance virtually the same. We argue that this is because deep subband filtering in the time-frequency domain fits the subband approximation often assumed in the dereverberation literature, whereas multiplicative masking corresponds to the narrowband approximation generally employed in denoising.

Index Terms: multi-frame filtering, subband approximation, dereverberation, denoising, neural network

1. Introduction

In modern communication devices, recorded speech is corrupted when clean speech sources are affected by interfering speakers, background noise and room acoustics. Speech restoration aims to recover clean speech from the corrupted signal, whereby two distinct tasks, denoising and dereverberation, are considered here [1, 2].

Traditional speech restoration algorithms are based on statistical methods, exploiting properties of the target and interfering signals to discriminate between them [3]. These include linear prediction [4], spectral enhancement [5], inverse filtering [6], and cepstral processing [7]. Modern approaches rely mostly on machine learning. In this field, predictive methods, learning a one-to-one mapping between corrupted and clean speech through a deep neural network (DNN), are most popular [8, 9]. A large portion of DNNs used in speech restoration are trained for mask estimation, i.e. they learn a mask value to be applied to each single bin of the signal, either in a learnt domain [10] or in the time-frequency (TF) domain [11, 12]. On the opposite, some approaches employ deep filtering [13], which means that their final stage involves a convolution between the input signal and a learnt multi-frame TF filter [14, 15, 16, 17, 18, 19, 20]. In [17], this filter is parameterized as a multi-frame MVDR [21] for denoising. A DNN-parameterized weighted prediction error subband filter is proposed in [19, 18, 20]. In [13, 14] it is directly learnt as a joint time- and frequency-filter, whereas in

[15] a frequency-independent time-dimension filter is learnt for subband filtering.

In this paper, we propose a deep subband filtering extension (DSFE) scheme to transform masking-based speech restoration DNNs into deep subband filters. The proposed extension is implemented by using a learnable temporal convolution at the output of the original masking DNN backbone and training the resulting architecture in an end-to-end fashion in the TF domain. Most of the time, the original masking DNN already handles multi-frame filtering internally through e.g. temporal convolutions. However, we show that enforcing explicit multi-frame subband filtering as the final stage of processing results in a significant performance increase for dereverberation while leaving the denoising performance virtually unaltered. We interpret our results and justify our approach by relating time-frequency multiplicative masking and deep subband filtering to the noising and reverberation corruption models respectively. The proposed approach has a negligible computational overhead and can be generically applied to any masking-based system.

The remainder of this paper is organized as follows. We first present an overview of the signal model and prerequisite assumptions for reverberation and noising corruptions. Then, we introduce our deep subband filtering extension scheme. We proceed with describing our experimental setup including data generation and training configuration. Finally we present and discuss our results.

2. Signal model

2.1. Narrowband and subband filtering

Filtering in the time-domain is obtained via convolution of a filter w with the speech signal s , yielding the filtered signal x :

$$x_t = \sum_{\tau} w_{\tau} s_{t-\tau}, \quad (1)$$

where t is the time index. A well-known result of Fourier theory is that, when transposed in the Fourier domain, such a filtering process can be expressed as a multiplication of the Fourier spectra. When using the short-time Fourier transform (STFT) however, the window used for analysis is of limited size, and spectral leakage between frequency bands can occur. Consequently, the true filtering model is:

$$\mathbf{x}_{t,f} = \sum_{\tau} \sum_{\nu} \tilde{\mathbf{w}}_{\tau,f,\nu} \mathbf{s}_{t-\tau,\nu}, \quad (2)$$

where f is the frequency index, $\mathbf{x} := \text{STFT}(x)$, $\mathbf{s} := \text{STFT}(s)$ and $\tilde{\mathbf{w}}_{\tau,f,\nu}$ is interpreted as a response to a time-frequency impulse $\delta_{\tau,f-\nu}$ [22]. The sum over index ν represents cross-band filtering, and the sum over index τ is a convo-

This work has been funded by the Federal Ministry for Economic Affairs and Climate Action, project 01MK20012S, AP380. The authors are responsible for the content of this paper.

lution along the time dimension.

The *subband approximation* ignores the effects of spectral leakage. Therefore, cross-band filtering is discarded and a single convolution is computed along the time-dimension in each frequency band independently:

$$\mathbf{x}_{t,f} = \sum_{\tau} \mathbf{w}_{\tau,f} \mathbf{s}_{t-\tau,f}, \quad (3)$$

where $\mathbf{w} := \text{STFT}(w)$.

The *narrowband approximation* further assumes that the length of the filter w is inferior to the STFT window length, therefore zeroing out the filter taps $\{\mathbf{w}_{\tau,f}; \tau \geq 1\}$ and yielding the following filtering model :

$$\mathbf{x}_{t,f} = \mathbf{w}_f \mathbf{s}_{t,f}. \quad (4)$$

2.2. Corruption models

Speech denoising consists in removing additive background noise n from the mixture x . The forward corruption process can naturally be represented in the STFT domain by addition of the clean speech and noise spectrograms:

$$\mathbf{x} = \mathbf{n} + \mathbf{s}. \quad (5)$$

Many speech denoising approaches use time-frequency masking, i.e. they compute a mask \mathbf{m} for each time-frequency bin and apply it to retrieve the clean speech estimate $\hat{\mathbf{s}}$:

$$\hat{\mathbf{s}}_{t,f} = (\mathbf{m} \odot \mathbf{x})_{t,f} := \mathbf{m}_{t,f}^t \mathbf{x}_{t,f}. \quad (6)$$

This model is similar to the narrowband approximation (4) with a *time-dependent* filter \mathbf{m} . We put the index t as superscript to avoid confusion with the time-convolution index τ .

In contrast to denoising, speech dereverberation aims to recover the anechoic speech corrupted by room acoustics. The signal model is exactly the filtering process in (1), where the filter w is called the room impulse response (RIR). Since the RIR length is almost always larger than the STFT window length, one cannot use the narrowband approximation (4) and has to resort to the subband approximation (3) instead. Consequently, some speech dereverberation methods perform inverse filtering in the STFT domain using the subband approximation [14, 4, 19, 18, 20]. That is, they try and estimate a filter $\bar{\mathbf{m}}$ supposed to represent the inverse of the RIR, such that the anechoic speech estimate is retrieved as:

$$\hat{\mathbf{s}}_{t,f} = (\bar{\mathbf{m}} *_{\tau} \mathbf{x})_{t,f} := \sum_{\tau} \bar{\mathbf{m}}_{t,f}^{\tau} \mathbf{x}_{t-\tau,f}. \quad (7)$$

Please note that in the model above in contrast to (3), the filter values $\bar{\mathbf{m}}$ are considered as *time-dependent*, same as in the time-frequency masking case. This is very often assumed in order to account for non-stationarity of the RIR and estimation errors [23, 18, 20, 24].

3. Deep subband filtering extension

Many neural network-based schemes use time-frequency masking, without examining the nature of the corruption. In this section, we present our DSFE scheme, which turns the time-frequency masks produced by such DNNs into subband filters. Let f_{θ} be a DNN providing a mask $\mathbf{m} = f_{\theta}(\mathbf{x})$ in the complex spectrogram domain, such that the clean spectrogram estimate is obtained via time-frequency masking (6).

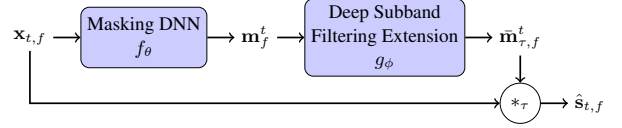


Figure 1: Proposed model diagram. The blue blocks are learnable neural networks.

We wish to extend the mask \mathbf{m} into a filter $\bar{\mathbf{m}}$ implemented by the neural network combination $\bar{\mathbf{m}} = g_{\phi}(f_{\theta}(\mathbf{x}))$, such that the clean estimate is obtained via subband filtering (7). Essentially, we want to turn masking DNNs into deep subband filters [13]. To this end, we design the *deep subband filtering extension* g_{ϕ} as a point-wise two-dimensional convolutional layer with tanh activation. The maps are of size $T \times F$, the kernels of size 1×1 and there are 2 input and $2N_f$ output channels corresponding to the single-frame mask and multi-frame filter real and imaginary parts, respectively:

$$g_{\phi} : \mathbf{m} \rightarrow \bar{\mathbf{m}} = \frac{1}{N_f} \tanh (\text{Conv2D}(\mathbf{m}; \phi)), \quad (8)$$

Note that we feed the spectrogram \mathbf{x} to the neural network and only use the multi-frame representation $\{\mathbf{x}_{t-\tau,f}; \tau \in [0, 1, \dots, N_f - 1]\}$ for filtering. This is because the multi-frame representation does not add any relevant information with respect to \mathbf{x} : since most DNNs compute correlations along the time-dimension already, it is redundant to provide a vector which explicitly encodes that time-delayed information. The proposed algorithm is summarized on Figure 1.

As the corresponding inverse filtering model better fits the corruption model for reverberation, we expect our DSFE method to perform better at dereverberation than its masking counterpart, and not to produce significant changes for denoising.

4. Experimental setup

4.1. Data

Both datasets for denoising and dereverberation experiments use the Wall Street Journal corpus (WSJ0, [25]) for clean speech sources. The training, validation and test splits comprise 101, 10 and 8 speakers for a total of 12777, 1206 and 651 utterances and a length of 25, 2.3 and 1.5 hours of speech respectively, sampled at 16kHz.

Speech Denoising: The WSJ0+Chime dataset is generated using clean speech extracts from the WSJ0 corpus and noise signals from the CHiME3 dataset [26]. The mixture signal is created by randomly selecting a noise file and adding it to a clean utterance with a signal-to-noise ratio (SNR) sampled uniformly between -6 and 14 dB.

Speech Dereverberation: The WSJ0+Reverb dataset is generated using clean speech data from the WSJ0 corpus and convolving each utterance with a simulated RIR. We use the `pyroomacoustics` library [27] to simulate the RIRs. The reverberant room is modeled by sampling uniformly a target T_{60} between 0.4 and 1.0 seconds and room length, width and height in $[5, 15] \times [5, 15] \times [2, 6]$ m. The anechoic target is generated using the T_{60} -shortening method [28], where the RIR is shaped by a decaying exponential window so that the resulting T_{60} equals 200ms. This results in an average direct-to-reverberation ratio (DRR) of -5.3 dB.

4.2. Single-frame DNN backbone

In this paper, we use the GaGNet architecture by [11], a state-of-the-art denoising neural network, which is the successor of [29] which ranked first in the real-time enhancement track of the DNS-2021 challenge. GaGNet leverages magnitude-only and complex-domain information in parallel with temporal convolutional networks. The rationale is to obtain a coarse estimation with the magnitude-processing "glance" modules, and to refine this estimation with "gaze" modules processing the real and imaginary parts of the complex spectrogram. Between each repeated glance and gaze module, an approximate complex ratio mask [12] is applied on the current version of the signal to enforce a coherent filtering process and stabilize training. Finally, the network outputs multiplicative mask values for the real and imaginary parts. We name our proposed method DSFE-GaGNet, which is the concatenation of GaGNet with the DSFE module g_ϕ . Although we focus on GaGNet in this work, please note that our DSFE method is compatible with any architecture performing mask estimation in the complex STFT domain. It could even be envisaged to use a similar extension in a different domain e.g. learnt by an DNN encoder, if subband filtering makes sense in that transform domain.

4.3. Training configuration

We use the same training configuration as GaGNet [11]: the STFT uses a Hann window with 320 points and 50% overlap at a sample rate of 16kHz. We employ square-root compression on the magnitude spectrogram. Therefore, the features that are fed to GaGNet are: $\text{cat}(\sqrt{|\mathbf{x}|} \cos(\phi_x), \sqrt{|\mathbf{x}|} \sin(\phi_x))$, where $\mathbf{x} = |\mathbf{x}| \exp(j\phi_x)$ is the noisy complex spectrogram. The training loss is a sum of mean square errors with respect to the real part, imaginary part and magnitude of the clean and estimated spectrograms. The networks are trained with the Adam optimizer with a learning rate of 0.005. Contrarily to [11], we use mini-batches of size 48 and use early stopping with a patience of 50 epochs and a maximum of 2000 epochs.

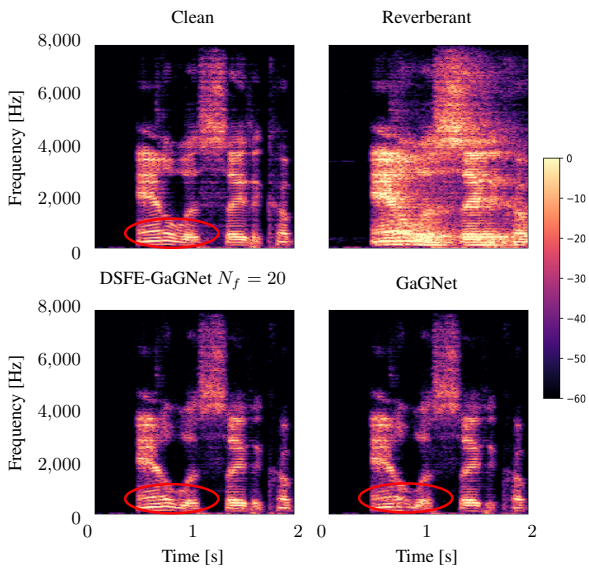


Figure 2: Log-energy spectrograms of clean, reverberant and processed signals from the WSJ0+Reverb dataset. The harmonic structure in the red circle is altered with GaGNet and better preserved with DSFE-GaGNet. $T_{60} = 0.85s$.

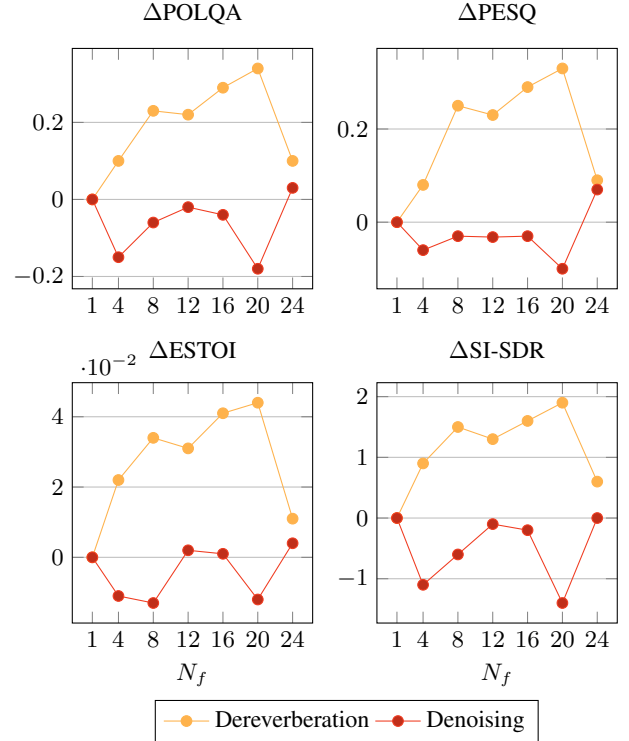


Figure 3: *Instrumental metrics improvements of DSFE-GaGNet with respect to single-frame GaGNet for speech denoising on WSJ0+Chime and dereverberation as a function of the number of frames N_f used for multiframe extension.*

4.4. Evaluation

We conduct instrumental evaluation using classical speech metrics like Perceptual Objective Listening Quality Analysis (POLQA) [30], Perceptual Evaluation of Speech Quality (PESQ) [31], Extended Short-Term Objective Intelligibility (ESTOI) [32] as well as scale-invariant (SI-) signal-to-distortion ratio (SDR), signal-to-interference ratio (SIR) and signal-to-artifacts ratio (SAR) [33]. We also report the number of million single-point floating operations per second of processed speech (MFLOPS·s⁻¹) as provided by the pypapi library¹.

5. Experimental results and discussion

5.1. Multi-frame filtering for speech enhancement tasks

We report results for dereverberation on WSJ0+Reverb and denoising on WSJ0+Chime in tables 1 and 2 respectively. For a more direct comparison, we group these experiments in Figure 3 by showing the improvements of DSFE-GaGNet with respect to its single-frame GaGNet counterpart as a function of N_f for both dereverberation and denoising.

For dereverberation, we observe a monotonic increase in all instrumental metrics as more frames are used in DSFE-GaGNet. The performance peaks at $N_f = 20$ with an improvement of .33 PESQ, .04 ESTOI and 1.9dB SI-SDR. The improvement over the single-frame version then decreases, as we observe that training is less stable with a high number of frames e.g. $N_f =$

¹<https://github.com/flozz/pypapi>

Table 1: Dereverberation results obtained on the WSJ0-Reverb dataset. Values indicate mean and standard deviation.

Method	N_f	POLQA	PESQ	ESTOI	SI-SDR	SI-SIR	SI-SAR	$\text{MFLOPS}\cdot\text{s}^{-1}$
Mixture	—	1.94 ± 0.40	1.51 ± 0.30	0.62 ± 0.12	1.2 ± 2.8	-0.8 ± 2.5	—	—
GaGNet	1	3.07 ± 0.43	2.52 ± 0.44	0.83 ± 0.06	6.0 ± 2.4	5.9 ± 2.6	6.0 ± 2.4	367.2
DSFE-GaGNet	4	3.17 ± 0.41	2.60 ± 0.44	0.85 ± 0.05	6.9 ± 2.3	6.8 ± 2.7	6.4 ± 2.2	368.6
DSFE-GaGNet	8	3.30 ± 0.42	2.77 ± 0.44	0.86 ± 0.05	7.5 ± 2.1	7.4 ± 2.7	6.7 ± 2.1	368.8
DSFE-GaGNet	12	3.29 ± 0.42	2.75 ± 0.44	0.86 ± 0.05	7.3 ± 2.2	7.1 ± 2.7	6.7 ± 2.2	370.0
DSFE-GaGNet	16	3.36 ± 0.42	2.81 ± 0.45	0.87 ± 0.05	7.6 ± 2.2	7.6 ± 2.7	6.7 ± 2.2	370.3
DSFE-GaGNet	20	3.41 ± 0.40	2.85 ± 0.44	0.87 ± 0.05	7.9 ± 2.3	7.9 ± 2.9	6.9 ± 2.2	371.6
DSFE-GaGNet	24	3.17 ± 0.43	2.61 ± 0.45	0.84 ± 0.06	6.6 ± 2.4	6.5 ± 2.7	6.2 ± 2.3	371.8

Table 2: Denoising results obtained on the WSJ0+Chime dataset. Values indicate mean and standard deviation.

Method	N_f	POLQA	PESQ	ESTOI	SI-SDR	SI-SIR	SI-SAR	$\text{MFLOPS}\cdot\text{s}^{-1}$
Mixture	—	2.08 ± 0.64	1.38 ± 0.32	0.65 ± 0.18	4.3 ± 5.8	4.3 ± 5.8	—	—
GaGNet	1	3.48 ± 0.60	2.75 ± 0.59	0.89 ± 0.08	15.5 ± 4.1	26.1 ± 4.5	16.0 ± 4.3	367.2
DSFE-GaGNet	4	3.33 ± 0.64	2.69 ± 0.59	0.88 ± 0.08	14.4 ± 4.1	25.2 ± 5.0	14.8 ± 4.2	368.6
DSFE-GaGNet	8	3.42 ± 0.63	2.72 ± 0.60	0.88 ± 0.08	14.9 ± 4.1	26.2 ± 4.8	15.4 ± 4.2	368.8
DSFE-GaGNet	12	3.46 ± 0.61	2.75 ± 0.58	0.89 ± 0.08	15.0 ± 4.0	27.0 ± 5.1	15.4 ± 4.0	370.0
DSFE-GaGNet	16	3.44 ± 0.63	2.72 ± 0.59	0.89 ± 0.08	15.3 ± 4.2	26.7 ± 4.8	15.7 ± 4.3	370.3
DSFE-GaGNet	20	3.30 ± 0.63	2.65 ± 0.57	0.88 ± 0.08	14.1 ± 3.9	24.7 ± 5.0	14.6 ± 3.9	371.6
DSFE-GaGNet	24	3.51 ± 0.60	2.82 ± 0.56	0.89 ± 0.08	15.5 ± 4.1	27.1 ± 4.8	16.0 ± 4.2	371.8

24. We observe on the spectrograms displayed in Figure 2 that DSFE-GaGNet preserves the harmonic structure in some cases where that structure is altered by GaGNet.

In the denoising case, the DSFE module reveals useless as DSFE-GaGNet performance saturates at the level of the single-frame GaGNet, or even worsens with more frames, at the exception of $N_f = 24$ where marginal improvements are observed.

This comparison suggests that subband filtering should be adopted when it fits the corruption model, i.e. for convolutive signal models like reverberation where the narrowband approximation requirements are not satisfied. In that case, we can obtain remarkable improvements at a very low computational cost: our best model DSFE-GaGNet with $N_f = 20$ only requires $4.4 \text{ MFLOPS}\cdot\text{s}^{-1}$ more than GaGNet, that is, a relative 1.2% increase. Furthermore, the temporal convolution used in the DSFE module with $N_f = 20$ frames employs only 96 trainable parameters, which is negligible compared to the 5.9M parameters of the original GaGNet backbone.

5.2. Ablation study

In Table 3 we present results of an ablation study showing various training strategies for DSFE-GaGNet. The default training configuration is denoted as *Join*, i.e. when both the DSFE module and the GaGNet backbone are trained jointly from scratch. We also try pretraining the GaGNet backbone and subsequently tuning the DSFE module parameters, either leaving the GaGNet backbone frozen (*Pretrain+Freeze*) or finetuning it along the DSFE parameters (*Pretrain+Finetune*). As expected, joint training performs best, but the improvement over *Pretrain+Finetune* is marginal. This highlights that it is paramount to jointly tune the DSFE parameters along with the single-frame backbone, at least at some stage of the training.

Table 3: Dereverberation results of DSFE-GaGNet on WSJ0+Reverb. All approaches use $N_f = 20$ frames. Values indicate mean and standard deviation.

Strategy	POLQA	ESTOI	SI-SDR
Mixture	1.94 ± 0.40	0.62 ± 0.12	1.2 ± 2.8
Pretrain+Freeze	3.19 ± 0.42	0.84 ± 0.06	6.8 ± 2.4
Pretrain+Finetune	3.40 ± 0.41	0.86 ± 0.05	7.5 ± 2.5
Join	3.41 ± 0.40	0.87 ± 0.05	7.9 ± 2.3

6. Conclusion

We present a deep subband filtering extension scheme transforming DNNs performing time-frequency multiplicative masking into deep subband filters. We show that such an extension fits the subband filtering approximation used for dereverberation in the STFT domain, while time-frequency masking fits the narrowband filtering approximation used for denoising. Consequently, we show that our deep subband filtering extension significantly increases dereverberation performance while leaving denoising performance virtually the same. The proposed extension scheme can be generically applied to any DNN baseline performing time-frequency masking. Ablation studies suggest that the deep subband filtering extension module should be trained jointly with the original single-frame DNN, at least at some stage of the training.

7. References

[1] P. Naylor and N. Gaubitch, *Speech Dereverberation*, vol. 59. Springer, Jan. 2011.

[2] S. J. Godsill, P. J. W. Rayner, and O. Cappé, *Digital audio restoration*. Springer, Sept. 1998.

[3] T. Gerkmann and E. Vincent, “Spectral masking and filtering,” in *Audio Source Separation and Speech Enhancement* (E. Vincent, ed.), John Wiley & Sons, 2018.

[4] T. Nakatani, T. Yoshioka, K. Kinoshita, M. Miyoshi, and B. Juang, “Blind speech dereverberation with multi-channel linear prediction based on short time fourier transform representation,” in *IEEE Int. Conf. Acoustics, Speech, Signal Proc. (ICASSP)*, (Las Vegas, USA), May 2008.

[5] E. Habets, *Single- and Multi-Microphone Speech Dereverberation Using Spectral Enhancement*. PhD thesis, Jan. 2007.

[6] I. Kodrasi, T. Gerkmann, and S. Doclo, “Frequency-domain single-channel inverse filtering for speech dereverberation: Theory and practice,” in *IEEE Int. Conf. Acoustics, Speech, Signal Proc. (ICASSP)*, (Florence, Italy), May 2014.

[7] T. Gerkmann, “Cepstral weighting for speech dereverberation without musical noise,” in *2011 19th European Signal Processing Conference*, (Barcelona, Spain), Sept. 2011.

[8] K. P. Murphy, *Probabilistic Machine Learning: Advanced Topics*. MIT Press, 2023.

[9] D. Wang and J. Chen, “Supervised speech separation based on deep learning: An overview,” *IEEE Trans. Audio, Speech, Language Proc.*, vol. 26, no. 10, pp. 1702–1726, 2018.

[10] Y. Luo and N. Mesgarani, “Conv-TasNet: Surpassing ideal time–frequency magnitude masking for speech separation,” *IEEE Trans. Audio, Speech, Language Proc.*, vol. 27, no. 8, pp. 1256–1266, 2019.

[11] A. Li, C. Zheng, L. Zhang, and X. Li, “Glance and gaze: A collaborative learning framework for single-channel speech enhancement,” *Applied Acoustics*, vol. 187, p. 108499, 2022.

[12] D. S. Williamson and D. Wang, “Time-frequency masking in the complex domain for speech dereverberation and denoising,” *IEEE/ACM Trans. Audio, Speech, Language Proc.*, vol. 25, no. 7, pp. 1492–1501, 2017.

[13] W. Mack and E. A. P. Habets, “Deep filtering: Signal extraction and reconstruction using complex time-frequency filters,” *IEEE Signal Proc. Letters*, vol. 27, pp. 61–65, 2020.

[14] H. Schröter, A. N. Escalante-B, T. Rosenkranz, and A. Maier, “DeepFilterNet: A low complexity speech enhancement framework for full-band audio based on deep filtering,” in *IEEE Int. Conf. Acoustics, Speech, Signal Proc. (ICASSP)*, (Singapore, Singapore), May 2022.

[15] H. Schröter, T. Rosenkranz, A. N. Escalante-B, M. Aubreville, and A. Maier, “Clcnet: Deep learning-based noise reduction for hearing aids using complex linear coding,” in *IEEE Int. Conf. Acoustics, Speech, Signal Proc. (ICASSP)*, pp. 6949–6953, 2020.

[16] S. Lv, Y. Hu, S. Zhang, and L. Xie, “DCCRN+: Channel-wise subband DCCRN with SNR estimation for speech enhancement,” in *Interspeech*, (Brno, Czech Republic), Sept. 2021.

[17] M. Tammen and S. Doclo, “Deep multi-frame MVDR filtering for single-microphone speech enhancement,” in *IEEE Int. Conf. Acoustics, Speech, Signal Proc. (ICASSP)*, (Toronto, Canada), May 2021.

[18] J. Heymann, L. Drude, R. Haeb-Umbach, K. Kinoshita, and T. Nakatani, “Frame-online DNN-WPE dereverberation,” in *Int. Workshop on Acoustic Echo and Noise Control (IWAENC)*, (Tokyo, Japan), Sept. 2018.

[19] K. Kinoshita, M. Delcroix, H. Kwon, T. Mori, and T. Nakatani, “Neural network-based spectrum estimation for online WPE dereverberation,” in *Interspeech*, (Stockholm, Sweden), Sept. 2017.

[20] J.-M. Lemercier, J. Thiemann, R. Koning, and T. Gerkmann, “Customizable end-to-end optimization of online neural network-supported dereverberation for hearing devices,” in *IEEE Int. Conf. Acoustics, Speech, Signal Proc. (ICASSP)*, (Singapore, Singapore), May 2022.

[21] Y. A. Huang and J. Benesty, “A multi-frame approach to the frequency-domain single-channel noise reduction problem,” *IEEE Trans. Audio, Speech, Language Proc.*, vol. 20, no. 4, pp. 1256–1269, 2012.

[22] Y. Avargel and I. Cohen, “System Identification in the Short-Time Fourier Transform Domain With Crossband Filtering,” *IEEE Trans. Audio, Speech, Language Proc.*, vol. 15, pp. 1305–1319, May 2007.

[23] A. Jukić, T. van Waterschoot, and S. Doclo, “Adaptive speech dereverberation using constrained sparse multichannel linear prediction,” *IEEE Signal Processing Letters*, vol. 24, no. 1, pp. 101–105, 2017.

[24] J.-M. Lemercier, J. Thiemann, R. Koning, and T. Gerkmann, “Neural Network-augmented Kalman Filtering for Robust Online Speech Dereverberation in Noisy Reverberant Environments,” in *Interspeech*, (Incheon, South Korea), Sept. 2022.

[25] J. S. Garofolo, D. Graff, D. Paul, and D. Pallett, “CSR-I (WSJ0 Complete),” *Linguistic Data Consortium*, May 2007.

[26] J. Barker, R. Marixer, E. Vincent, and S. Watanabe, “The third CHiME speech separation and recognition challenge: Dataset, task and baselines,” in *IEEE Workshop on Automatic Speech Recognition and Understanding (ASRU)*, (Scottsdale, USA), Dec. 2015.

[27] I. D. R. Scheibler, E. Bezzam, “Pyroomacoustics: A Python package for audio room simulations and array processing algorithms,” in *IEEE Int. Conf. Acoustics, Speech, Signal Proc. (ICASSP)*, (Calgary, Canada), Apr. 2018.

[28] R. Zhou, W. Zhu, and X. Li, “Speech dereverberation with a reverberation time shortening target,” *arXiv*, 2022.

[29] A. Li, W. Liu, X. Luo, C. Zheng, and X. Li, “ICASSP 2021 Deep Noise Suppression Challenge: Decoupling magnitude and phase optimization with a two-stage deep network,” in *IEEE Int. Conf. Acoustics, Speech, Signal Proc. (ICASSP)*, (Brno, Czech Republic), June 2021.

[30] ITU-T Rec. P.863, “Perceptual objective listening quality prediction,” *Int. Telecom. Union (ITU)*, 2018.

[31] A. Rix, J. Beerends, M. Hollier, and A. Hekstra, “Perceptual evaluation of speech quality (PESQ)-a new method for speech quality assessment of telephone networks and codecs,” in *IEEE Int. Conf. Acoustics, Speech, Signal Proc. (ICASSP)*, (Salt Lake City, USA), May 2001.

[32] J. Jensen and C. H. Taal, “An algorithm for predicting the intelligibility of speech masked by modulated noise maskers,” *IEEE/ACM Trans. Audio, Speech, Language Proc.*, vol. 24, no. 11, pp. 2009–2022, 2016.

[33] J. L. Roux, S. Wisdom, H. Erdogan, and J. R. Hershey, “SDR - half-baked or well done?,” in *IEEE Int. Conf. Acoustics, Speech, Signal Proc. (ICASSP)*, (Brighton, United Kingdom), May 2019.